

**METEOSAT
SECOND
GENERATION**

**MSG-1/SEVIRI Solar Channels Calibration
Commissioning Activity Report**



Doc.: EUM/MSG/TEN/04/0024
Issue: VERSION 1.0
Date: 21 Jan 2004

**MSG-1/SEVIRI Solar Channels Calibration
Commissioning Activity Report**

EUM/MSG/TEN/04/0024

Prepared by Y. Govaerts and M. Clerici

EUMETSAT

Am Kavalleriesand 31, Postfach 10 05 55, D-64205 Darmstadt, Germany
Tel: +49 6151 807345 * Fax: + 49 6151 807555

METEOSAT SECOND GENERATION	SEVIRI Solar Channels Calibration Commissioning Activity Report	 EUMETSAT Doc.: EUM/MSG/TEN/04/0024 Issue: VERSION 1.0 Date: 21 Jan 2004
---	--	---

Table of Contents

Table of Contents	ii
List of Acronyms	iii
1 INTRODUCTION	1
2 SEVIRI SOLAR CHANNELS CHARACTERISTICS	2
3 CALIBRATION METHOD OVERVIEW	3
3.1 General concept	3
3.2 Target Identification	4
3.3 Calibration	5
3.3.1 Calibration of individual observations	5
3.3.2 Temporal averaging	5
3.3.3 Spatial averaging	5
3.3.4 Final consistency check	5
4 COMMISSIONING CALIBRATION ACTIVITY RESULTS	7
4.1 Test organisation	7
4.2 Calibration periods	7
4.3 Calibration coefficient estimation	7
4.4 IQGSE/IMPF comparison	10
4.5 Calibration error estimation	10
4.6 Desert and sea target calibration coefficient consistency	11
4.7 Retrieved space count	12
5 VALIDATION	14
5.1 Radiance simulation accuracy estimation	14
5.2 Comparison with CERES	16
6 APPLYING THE CALIBRATION COEFFICIENTS	17
7 CONCLUSION	18
References	18
Annex	20
A HRVIS SPECTRAL RESPONSE USED IN SSCC	21
B ERROR BUDGET OVER SEA TARGETS	23
C METEOSAT-7 ERROR BUDGET	24
D CALIBRATION RESULTS OVER EACH TARGET	25

List of Acronyms

AOT	Aerosol Optical Thickness
AU	Astronomical Unit
BRF	Bidirectional Reflectance Factor
DC	Digital Count
IQGSE	Image Quality Ground Segment Equipment
IMPF	IMage Processing Facility
MSG	Meteosat Second Generation
NIR	Near-Infrared
NSR	Normalized Spectral Response
QI	Quality Indicator
RMIB	Royal Meteorological Institute of Belgium
RTM	Radiative Transfer Model
SNR	Signal to Noise Ratio
SEVIRI	Spinning Enhanced Visible and InfraRed Imager
SSCC	SEVIRI Solar Channel Calibratrion
SZA	Sun Zenith Angle
U-MARF	Unified Meteorological Archive Facility

METEOSAT SECOND GENERATION	SEVIRI Solar Channels Calibration Commissioning Activity Report	 Doc. : EUM/MSG/TEN/04/0024 Issue: VERSION 1.0 Date : 21 Jan 2004
---	--	---

1 INTRODUCTION

This document describes the results of the SEVIRI solar channel (namely, HRV, VIS0.6, VIS0.8 and IR1.6) calibration activities that took place during MSG-1 commissioning period. SEVIRI Calibration Validation Plan (Müller 2003) foresees a series of four tests listed below:

Testing activity	Description
CVT-TT-SSCCVA-ACDATA	Data Acceptance Verification
CVT-TT-SSCCVA-LIFE	SSCC Functionality Verification
CVT-CO-WARMCH-BIASSCCAPPLICATION	Core Warm Channel Calibration Validation
CVT-LT-WARMCH-BIASSCCAPPLICATION	Long-term Warm Channel Calibration Validation

This document covers only testing activity CVT-CO-WARMCH-BIASSCCAPPLICATION. The objective of this activity is to derive calibration coefficients with a accuracy of $\pm 10\%$ during the commissioning period whereas the objective of activity CVT-LT-WARMCH-BIASSCCAPPLICATION is to monitor the sensor drift and to derive calibration coefficient with $\pm 5\%$ accuracy.

The calibration is performed with the SSCC software which is running as a stand-alone facility in the MSG ground segment. The calibration method is briefly described in Section (3). The results of the calibration tests are presented in Section (4). The validation of these results are described in Section (5).

Section (6) describes how to apply the calibration coefficients stored in the SEVIRI level 1.5 file header to the digital count value.

2 SEVIRI SOLAR CHANNELS CHARACTERISTICS

The East-West and South-North sampling distance at the sub-satellite point is 3×3 km (1×1 km for HRV), and the instantaneous field of view is about 5km (2km for HRV). The characteristics of the channels located in the solar spectral region are given in Table (1), where the pre-launch radiometric performances are given for the SEVIRI instrument onboard MSG-1. The actual post-launch SNR performances estimated on 28 May 2003 are within the specifications. Each spectral channel is composed of three detectors, except HRV with nine. The output signal of all channels is coded on 10 bits. The normalized spectral response $\xi(\lambda)$ of the solar channels is characterized with a mean relative error of about 1%, which represents a significant improvement with respect to the VIS band of the Meteosat first generation radiometer. The characterization of the HRVIS band between 0.40 and $0.45\mu\text{m}$ has been taken from SEVIRI Flight Model 3, forcing the response of this latter instrument to match the original one at $0.45\mu\text{m}$. Values below 0.40 and above $1.05\mu\text{m}$ have been extrapolated. The actual HRVIS NSR values used in SSCC are listed in Annex (A). The sensor normalized spectral responses (NSR) and associated error are shown on Fig. (1). The NSR total error accounts for errors due to the absolute wavelength calibration uncertainty, the measurement noise and bias of the optic and detector transmittance.

The radiometric preprocessing of level 1.0 data, *i.e.*, the transformation of raw data to level 1.5 geo-located radiances, includes the linearization of the signal, the equalization of the detector output of a same channel and finally the pixel geo-location to a reference grid centered at 0 degree longitude (Schmetz et al. 2002). The image size is 3712×3712 pixels except for the HRV band which has a size of 11136×5568 (SN \times EW). The geo-location absolute accuracy is expected to be about one pixel with a root mean square error from image to image less than 0.5 pixel. Ground control points are used to monitor the quality of the geo-location process.

Channel	Spectral Band (μm)	Dynamic Range	Short-term SNR Spec.	SNR Perf.	NSR std. d.	Cal. Requ.
VIS0.6	0.56 – 0.71	0 – 533	SNR > 10.1	610	1.0%	10.66
VIS0.8	0.74 – 0.88	0 – 357	SNR > 7.3	70	1.0%	7.14
NIR1.6	1.50 – 1.78	0 – 75	SNR > 3.0	11	0.8%	1.50
HRV	0.37 – 1.25	0 – 460	SNR > 4.3	2.5	1.8%	9.18

Table 1: SEVIRI Solar Channel Characteristics. The dynamic range is given in $\text{W m}^{-2} \text{sr}^{-1} \mu\text{m}^{-1}$. The Signal to Noise Ratio (SNR) is given at 1% of the maximum dynamic range. The standard deviation (std. d.) of the Normalized Spectral Response (NSR) specification is given in percent. The calibration requirement is given in $\text{W m}^{-2} \text{sr}^{-1} \mu\text{m}^{-1}$.

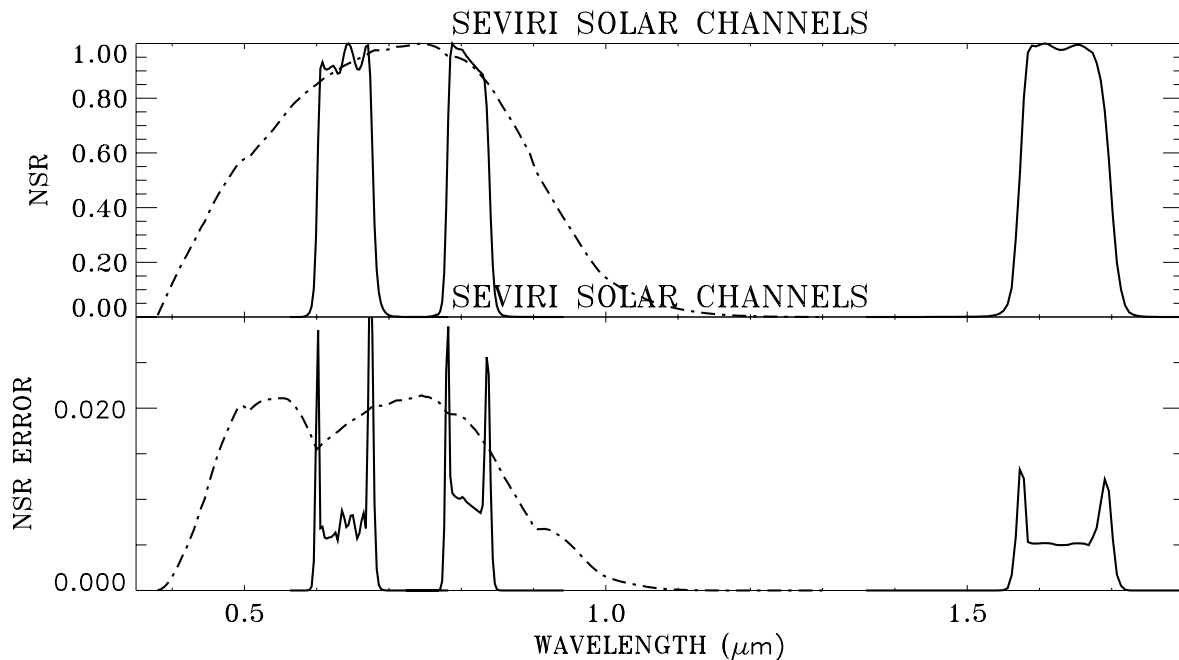


Figure 1: Top: Normalized Spectral Response (NSR) of the SEVIRI solar channels. The response of the HRV band is shown with a dash-dotted line. Bottom: NSR characterization absolute error.

3 CALIBRATION METHOD OVERVIEW

3.1 General concept

As there is no on board calibration device for the solar channels, their calibration rely on a vicarious method based radiative transfer modelling over bright desert surfaces as primary calibration target type. Targets located over sea surfaces are used to verify the consistency and reliability of the results. This method has been implemented in the SSCC algorithm which is designed to minimize the error propagation while deriving a calibration coefficient and to verify the consistency of this estimation. This mechanism requires the processing of a large amount of images to derive a reliable calibration error. Additionally, the processing of a many images should permit to reduce the errors, provided that these errors are independent and random, *i.e.*, not systematic. An error reduction methods has thus been developed and relies on a twofold strategy. Firstly, a target identification process aims at finding cases where the target parameter error is minimum. Secondly, an error reduction based on temporal and spatial averaging of the results is applied to detect inconsistent results, if any, and to reduce the effects due to random errors. It is therefore necessary to discriminate systematic from random errors. As atmospheric properties are essentially controlled by the aerosol load prescribed from a climate data set, uncertainty of these parameters are responsible for systematic errors in time, *i.e.*, over a same target. Similarly, since desert target properties are very stable, any uncertainty in the characterization of these properties are also responsible for systematic errors in time. Both type of parameters are however not spatially correlated. All errors are estimated for a given confidence level set to 95%.

3.2 Target Identification

For each analyzed image during a processing period, an identification process takes place to select potential targets whose actual properties and observation/illumination angles correspond to cases where calculated radiance error is minimum. Over desert targets, cloud and sand storm cases are identified analyzing daily variations of the observed count values. Clear sky pixel detection is performed both with a threshold method and fitting a second order polynomial to the daily cycle of observations. Any deviation from this polynomial is interpreted as a cloud contamination, cloud shadow or sand storm. Observations of that day are disregarded when the remaining number of clear sky slots is too low after this daily filtering. Sea targets are defined by large search areas in which cloud and aerosol free potential pixels are identified, looking at uniform and very low digital count values outside the sun-glint regions. This procedure is used to ensure a very low aerosol optical thickness.

When a target is successfully identified within an image acquired at time t , the $N_c \times N_l$ pixels centered on the target location are extracted from the corresponding image. The average value, minimum, maximum and error of the observed pixel count values over that site are next evaluated. The associated radiometric error is estimated at 95% confidence level accounting for both the instrument noise and any deviation from the target uniformity. Since targets are very uniform areas, the difference between the maximum and minimum count value within the target are expected to be very small. An observation is rejected when it is not the case.

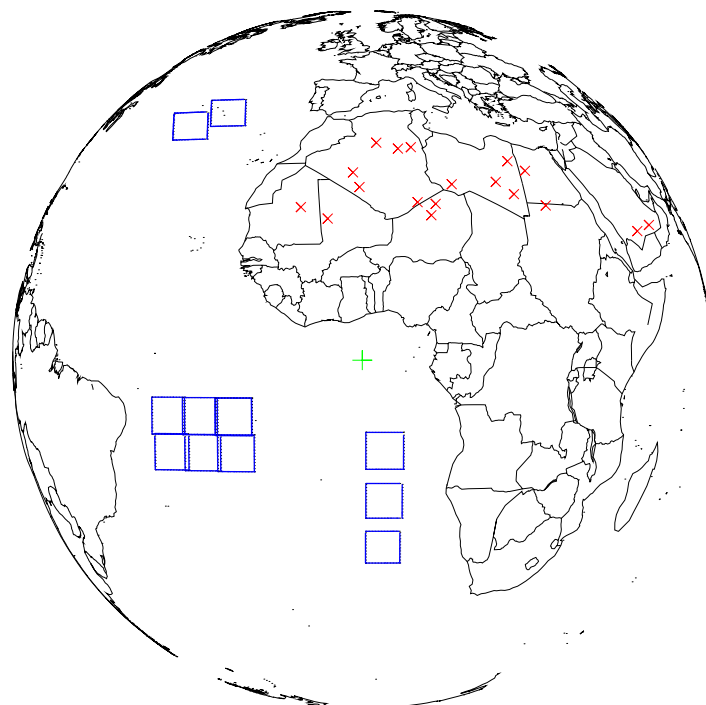


Figure 2: Location of the calibration targets for the 0° nominal sub-satellite position, shown with green “+” symbol. Desert target locations are indicated with the red \times symbol and sea search areas with blue boxes.

3.3 Calibration

3.3.1 Calibration of individual observations

For all successfully identified targets, TOA radiances are calculated with the 6S code (Vermote et al. 1997) accounting for the illumination and viewing angles at the acquisition time and the surface and atmospheric properties. Simulated radiance errors are due to individual state variable error and the Radiative Transfer Model (RTM) intrinsic error, *i.e.*, imprecision of the numerical procedure not related to errors in the model input parameters (Koepke 1982). Finally, the effective radiance is affected both by the uncertainty on the sensor spectral response characterization.

The time series composed of pairs of observed count / simulated radiance are accumulated individually for each target during the period. A calibration coefficient is estimated for each pair of the time series. The corresponding error is expressed as the quadratic sum of the relative radiance *i.e.*, surface and atmospheric parameterization error, RTM intrinsic error, NSR error and radiometric errors.

3.3.2 Temporal averaging

Only the instrument radiometric noise is responsible for temporal random errors. Calibration coefficients derived over each target are thus temporally averaged to reduce random error effects due to radiometric noises. An additional test is performed to verify the consistency of the mean coefficients derived over each desert targets. Simulation reliability is controlled exploiting the anisotropy signature of the surface responsible for observed count variations (Govaerts et al. 1998). Calculated radiance daily variations are thus compared with observations. When both simulation and observation are consistent, it should be possible to retrieve the offset value. This retrieved offset value is compared with the actual one, derived from deep space observations. When the surface BRF and/or the aerosol load are not correct, simulated radiance corresponding to high Sun Zenith Angles (SZAs) might exhibit systematic biases with respect to those calculated for low (SZAs). Such situation will be responsible for an erroneous retrieval of the offset.

3.3.3 Spatial averaging

All the coefficients temporally averaged over each target are spatially averaged, assuming that the surface and atmosphere characterization errors are not correlated. Since spectral properties of desert targets are quite similar, these coefficients should normally be very close, even in case of large errors in the characterization of the sensor response. Hence, outliers, if any, are expected to result from modelling errors and are disregarded. The calibration coefficient error is estimated assuming that the surface and atmosphere errors are not correlated as previously discussed.

3.3.4 Final consistency check

A final test is performed to verify the consistency of the final calibration coefficients and its associated error. To this end, calibration coefficients are derived over sea in a similar way to the exception of the daily cycle analysis which is not applied. Calibration coefficients derived over desert and sea

targets should be similar if i) the radiometer responds linearly to the incoming radiance intensity, ii) the characterization of the NSR is correct and finally iii) the radiative transfer simulations are reliable. When these conditions are met, the difference between the calibration coefficients derived over each target type should be smaller than the corresponding error. Still, the coefficients derived over desert and sea targets might be very close but affected by a similar bias. An additional test is therefore applied to verify the consistency of the results, based on a similar reasoning as in Section (3.3.2) to retrieve the space counts. This test is performed accounting for all the observations over both sea and desert that have successfully passed all the previous consistency checks.

4 COMMISSIONING CALIBRATION ACTIVITY RESULTS

4.1 Test organisation

Commissioning activity CVT-CO-WARMCH-BIASSCCAPPLICATION includes the following tests:

- Calibration coefficient estimation;
- Consistency of calibration coefficients derived from IQGSE and IMPF images;
- Calibration error budget estimation;
- Consistency between calibration over sea and desert targets;
- Retrieved space count consistency.

The results presented in this report have been generated with SSCC product number 08.06.01, which corresponds to the SSCC software release 3.06. Calibration coefficients have been derived from SEVIRI level 1.5 images processed either by IQGSE or IMPF and delivered by U-MARF.

4.2 Calibration periods

The calibration commissioning activity is based on the analysis of the following periods:

PERIOD	NBR DAYS	LEVEL 1.5
2003 054–055	2	IQGSE
2003 073–075	3	IQGSE
2003 086–087	2	IQGSE
2003 199–204	5	IQGSE
2003 216–220	5	IQGSE
2003 216–220	5	IMPF
2003 234–238	5	IMPF
2003 241–245	5	IMPF
2003 275–279	5	IMPF
2003 302–306	5	IMPF

Full 5 days calibration periods have been available only from Julian day 199. Most of the results analysis is therefore based on IMPF data received from July 2003.

4.3 Calibration coefficient estimation

The purpose if this first series of tests was to make sure SSCC can handle SEVIRI level 1.5 images and produce calibration coefficients.

The method presented in Section (3) has been applied to derive calibration coefficients and error for each solar channel during the commissioning periods. SSCC has been successfully applied on each selected calibration period. Results are shown on Figure (3) and in Table (2).

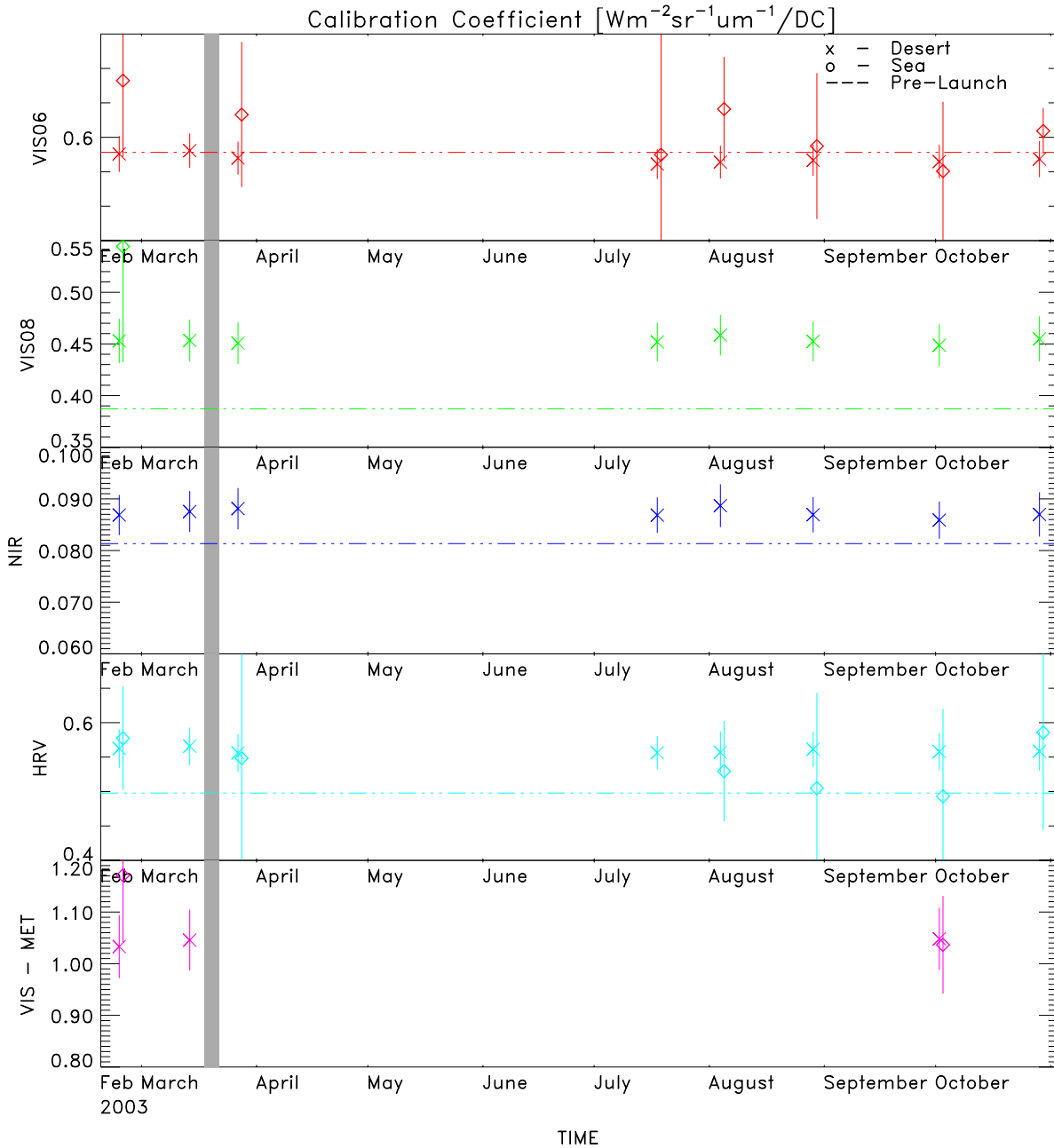


Figure 3: Overall results during the commissioning period. Pre-launch calibration coefficients are shown with the horizontal dash-dotted line. The \times symbol represents the calibration coefficient derived over desert targets. The \diamond symbol represents the calibration coefficient derived over sea targets. The shaded area corresponds to the decontamination of SEVIRI. Meteosat-7 calibration coefficients are given in $\text{Wm}^{-2}\text{sr}^{-1}/\text{DC}$.

METEOSAT SECOND GENERATION	SEVIRI Solar Channels Calibration Commissioning Activity Report	 EUMETSAT
		Doc.: EUM/MSG/TEN/04/0024 Issue: VERSION 1.0 Date : 21 Jan 2004

VIS06							
PERIOD	CAL. COEFF	REL. ERR.	RET. OFF.	SEA	SEA R. ERR.	DIFF	QI
2003 054 – 055	0.576	4.5	45.4	0.682	16.2	18.5	0.00
2003 073 – 075	0.581	4.3	44.0	0.000	0.0	0.0	0.05
2003 086 – 087	0.570	4.2	48.0	0.633	16.6	11.1	0.02
2003 199 – 204	0.561	3.9	52.9	0.575	143.6	2.4	0.28
2003 216 – 220	0.564	4.2	47.8	0.641	11.8	13.6	0.02
2003 241 – 245	0.567	4.0	48.7	0.587	18.1	3.6	0.31
2003 275 – 279	0.565	4.3	51.5	0.551	18.2	-2.5	0.36
2003 302 – 306	0.568	4.6	48.8	0.609	5.4	7.2	0.04
VIS08							
PERIOD	CAL. COEFF	REL. ERR.	RET. OFF.	SEA	SEA R. ERR.	DIFF	QI
2003 054 – 055	0.453	4.7	46.6	0.544	20.6	20.2	0.03
2003 073 – 075	0.453	4.4	46.5	0.000	0.0	0.0	0.12
2003 086 – 087	0.451	4.5	46.9	0.000	0.0	0.0	0.18
2003 199 – 204	0.452	4.1	52.5	0.000	0.0	0.0	0.30
2003 216 – 220	0.459	4.3	50.0	0.000	0.0	0.0	0.41
2003 241 – 245	0.453	4.3	47.7	0.000	0.0	0.0	0.14
2003 275 – 279	0.449	4.5	50.3	0.000	0.0	0.0	0.38
2003 302 – 306	0.455	4.8	44.3	0.000	0.0	0.0	0.02
NIR							
PERIOD	CAL. COEFF	REL. ERR.	RET. OFF.	SEA	SEA R. ERR.	DIFF	QI
2003 054 – 055	0.087	4.5	50.5	0.000	0.0	0.0	0.48
2003 073 – 075	0.088	4.5	46.3	0.000	0.0	0.0	0.24
2003 086 – 087	0.088	4.5	45.3	0.000	0.0	0.0	0.21
2003 199 – 204	0.087	4.0	55.1	0.000	0.0	0.0	0.19
2003 216 – 220	0.089	4.7	43.1	0.000	0.0	0.0	0.12
2003 241 – 245	0.087	3.9	50.7	0.000	0.0	0.0	0.48
2003 275 – 279	0.086	4.2	52.7	0.000	0.0	0.0	0.39
2003 302 – 306	0.087	4.9	47.4	0.000	0.0	0.0	0.27
HRV							
PERIOD	CAL. COEFF	REL. ERR.	RET. OFF.	SEA	SEA R. ERR.	DIFF	QI
2003 054 – 055	0.562	5.0	49.6	0.577	13.0	2.6	0.25
2003 073 – 075	0.566	4.8	47.7	0.000	0.0	0.0	0.23
2003 086 – 087	0.556	4.9	45.1	0.548	96.9	-1.4	0.13
2003 199 – 204	0.556	4.4	53.4	0.000	0.0	0.0	0.20
2003 216 – 220	0.557	5.4	52.9	0.530	13.8	-4.9	0.16
2003 241 – 245	0.561	4.5	54.5	0.505	27.4	-10.1	0.12
2003 275 – 279	0.558	4.9	51.3	0.493	25.8	-11.6	0.45
2003 302 – 306	0.558	5.0	46.5	0.586	24.3	4.9	0.08

Table 2: Major calibration results during the commissioning period for the SEVIRI solar channels band. The calibration coefficient is expressed in $\text{Wm}^{-2}\text{sr}^{-1}\mu\text{m}^{-1}/\text{DC}$, the error and the difference between desert and sea calibration in percent.

The difference between calibration over desert and sea is calculated with $DIFF = 100(SEA - DES)/DES$. A Quality Indicator (QI) lower than 0.05 indicates the calibration results are not reliable. As can be seen, the estimated error is below 5% to the exception of period 216–220 for the HRVIS band (see Section 4.5 for additional information). The calibration coefficients are fairly stable, indicating the SEVIRI solar channels are not suffering from any unexpected degradation. Calibration over sea targets in the VIS08 and NIR band does not take place because the simulation error are too large and the results not reliable at all. Details on calibration results over each target is shown in Annex (D) and on the error estimation in Section (4.5).

4.4 IQGSE/IMPF comparison

The purpose of this test is to verify the consistency of the calibration coefficients derived from Level 1.5 images generated by IQGSE and IMPF facilities respectively. This test has been applied on period 216–220. IMPF includes additional processing steps in the generation of the level 1.5 images such as the linearization and equalization of the signal from the various detectors. During that period, the following calibration coefficients have been derived (in $\text{Wm}^{-2}\text{sr}^{-1}\mu\text{m}^{-1}/\text{DC}$):

BAND	IQGSE	IMPF	REL. DIFF.
VIS06	0.571	0.564	-1.26
VIS08	0.464	0.459	-1.18
NIR	0.890	0.089	-0.34
HRVIS	0.569	0.557	-2.13

Note that the slots actually available from the two processing chain were not the same (many IQGSE slots were missing). The relative difference is estimated as $100(IMPF - IQGSE)/IQGSE$. This difference is about 1%, but in the HRVIS band. This difference is similar to the random noise of the SSCC calibration method (see Next Section) to the exception of the HRVIS band, where the difference between IMPF and IQGSE exceeds by 1% the random error contribution.

4.5 Calibration error estimation

The purpose of this test is to estimate the error budget in each solar channel and to analyze the error reduction during the various SSCC processing steps. When a calibration coefficient is derived over a single observation (see Section 3.3.1), the total error contribution is due to:

The error on the atmospheric parameters [ATM]

The error on the surface parameters [SRF]

The intrinsic RTM error [RTM]

The NSR characterization error [NSR]

The radiometric error [NOISE]

Since the radiometric error is assumed not correlated in time, the temporal averaging (see Section 3.3.2) over each target results in a change of the radiometric error into a random noise so that the remaining error contributions are:

The error on the atmospheric parameters

The error on the surface parameters

The intrinsic RTM error

The NSR characterization error

The random error

Atmospheric and surface parameter errors are assumed not spatially correlated so that the remaining error contribution after the spatial averaging (see Section 3.3.3) are:

The intrinsic RTM error

The NSR characterization error

The random error

	ATM	SRF	RTM	NSR	NOISE	RAND.	TOT.
DESERT VIS06							
OBSERV. $\delta_r c_f$	2.2	11.3	3.7	1.3	0.4		12.3
TIME AVG. $\delta_r \bar{c}_f$	2.2	10.9	3.6	1.2		0.5	11.8
SPACE AVG. $\delta_r \hat{c}_f$			3.6	1.2		0.9	3.9
DESERT VIS08							
OBSERV. $\delta_r c_f$	2.3	7.9	3.7	1.8	0.5		9.3
TIME AVG. $\delta_r \bar{c}_f$	2.5	7.9	3.7	1.7		0.6	9.3
SPACE AVG. $\delta_r \hat{c}_f$			3.7	1.7		1.1	4.3
DESERT NIR							
OBSERV. $\delta_r c_f$	1.3	12.2	2.8	0.6	0.5		13.0
TIME AVG. $\delta_r \bar{c}_f$	1.9	8.5	3.7	0.8		0.5	9.6
SPACE AVG. $\delta_r \hat{c}_f$			3.7	0.8		1.0	3.9
DESERT HRV							
OBSERV. $\delta_r c_f$	2.0	11.7	3.6	2.2	0.3		12.7
TIME AVG. $\delta_r \bar{c}_f$	2.1	11.8	3.7	2.2		0.5	12.8
SPACE AVG. $\delta_r \hat{c}_f$			3.7	2.2		1.4	4.5

Table 3: Relative error (%) contribution on the estimation of the calibration coefficient over desert targets.

The results of these error budgets are given in Table (3) over desert targets. The mean estimated error derived in each band is close to 4%. Results over sea targets are given in Annex (B).

The Meteosat-7 calibration error budget is given for information in Annex (C). The improvement of HRVIS with respect to the Meteosat VIS band translates in a much lower radiometric noise in particular of sea surface and a NSR error contribution twice smaller.

4.6 Desert and sea target calibration coefficient consistency

The purpose of this test is to verify the reliability of the SSCC RTM, the consistency of radiometric NSR characterization and finally the linearity of the solar channels. These tests are performed within the accuracy of SSCC.

If the SEVIRI instrument responds linearly to the incoming radiance and the NSR is correctly characterized, it is expected that the differences between calibration coefficients derived over sea and desert targets do not exceed their respective error at the 95% confidence level. This test is only possible for the VIS06 and HRVIS band. As can be seen on Table (2), this difference is lower than $\pm 5\%$ and $\pm 10\%$ for the VIS06 and HRVIS band respectively when the QI is bigger than 0.05. Half of this difference might be explained by the error on the NSR characterization. Calibration over sea and desert targets are thus consistent in these two bands.

In other words, within the SSCC accuracy limit, it has not been possible to detect any anomaly in the NSR characterization and the linearity of the HRVIS and VIS06 bands with this test.

4.7 Retrieved space count

The purpose of this test is to verify the reliability of the SSCC RTM and calibration procedure against the linearity of the instrument and the offset (space count) characterization. Offset value is fixed to 51 DC in all solar channels.

This test relies on a space count retrieval with a linear regression between the observed count values and the corresponding simulated radiance. It is part of the SSCC quality control tests. The slope (L. COEF) of this line should be similar to the estimated calibration coefficient (COEF) and its intercept with the X axis should give the retrieved offset (R. OFF.). The probability that these two values are equal is estimated at the 95% confidence level. Results of this test is given below in Table (4).

As can be seen, the estimated accuracy of the retrieved space count is different for each band and application cycle, but remains most of the time between $\pm 5\%$. This test does not reveal systematic problem in the retrieval of the space count value.

In other words, within the SSCC accuracy limit, it has not been possible to detect any anomaly in the offset characterization and the linearity of the SEVIRI solar channels with this test.

METEOSAT SECOND GENERATION	SEVIRI Solar Channels Calibration Commissioning Activity Report	 EUMETSAT Doc.: EUM/MSG/TEN/04/0024 Issue: VERSION 1.0 Date: 21 Jan 2004
---	--	---

VIS06								
PERIOD	OFF.	OFF. E.	R. OFF.	R OFF. E.	DIFF	PROB	COEF	L. COEF
2003 054 – 055	51.0	0.6	45.4	4.5	-11.0	0.01	0.576	0.563
2003 073 – 075	51.0	0.6	44.0	9.7	-13.8	0.10	0.581	0.565
2003 086 – 087	51.0	0.6	48.0	3.0	-6.0	0.04	0.570	0.563
2003 199 – 204	51.0	0.6	52.9	6.0	3.6	0.56	0.561	0.564
2003 216 – 220	51.0	0.6	47.8	2.4	-6.4	0.01	0.564	0.559
2003 241 – 245	51.0	0.6	48.7	2.1	-4.6	0.03	0.567	0.562
2003 275 – 279	51.0	0.6	51.5	2.6	1.0	0.73	0.565	0.565
2003 302 – 306	51.0	0.6	48.8	2.2	-4.4	0.05	0.568	0.563
VIS08								
PERIOD	OFF.	OFF. E.	R. OFF.	R OFF. E.	DIFF	PROB	COEF	L. COEF
2003 054 – 055	51.0	0.6	46.6	4.8	-8.5	0.06	0.453	0.445
2003 073 – 075	51.0	0.6	46.5	8.2	-8.8	0.24	0.453	0.446
2003 086 – 087	51.0	0.6	46.9	9.3	-8.0	0.36	0.451	0.444
2003 199 – 204	51.0	0.6	52.5	5.3	2.8	0.60	0.452	0.454
2003 216 – 220	51.0	0.6	50.0	8.3	-1.9	0.81	0.459	0.457
2003 241 – 245	51.0	0.6	47.7	6.6	-6.6	0.28	0.453	0.447
2003 275 – 279	51.0	0.6	50.3	5.3	-1.5	0.77	0.449	0.447
2003 302 – 306	51.1	0.6	44.3	7.2	-13.2	0.04	0.455	0.442
NIR								
PERIOD	OFF.	OFF. E.	R. OFF.	R OFF. E.	DIFF	PROB	COEF	L. COEF
2003 054 – 055	51.0	0.6	50.5	22.9	-1.0	0.96	0.087	0.087
2003 073 – 075	51.0	0.6	46.3	14.3	-9.2	0.48	0.088	0.086
2003 086 – 087	51.0	0.6	45.3	15.4	-11.2	0.41	0.088	0.087
2003 199 – 204	51.0	0.6	55.1	8.3	8.0	0.37	0.087	0.088
2003 216 – 220	51.0	0.6	43.1	15.6	-15.6	0.24	0.089	0.087
2003 241 – 245	51.0	0.6	50.7	10.9	-0.7	0.95	0.087	0.087
2003 275 – 279	51.1	0.6	52.7	11.1	3.1	0.79	0.086	0.086
2003 302 – 306	51.0	0.6	47.4	12.6	-7.1	0.54	0.087	0.086
HRV								
PERIOD	OFF.	OFF. E.	R. OFF.	R OFF. E.	DIFF	PROB	COEF	L. COEF
2003 054 – 055	51.0	0.6	49.6	4.2	-2.8	0.49	0.562	0.558
2003 073 – 075	51.0	0.6	47.7	9.2	-6.4	0.46	0.566	0.557
2003 086 – 087	51.0	0.6	45.1	11.5	-11.6	0.26	0.556	0.540
2003 199 – 204	51.0	0.6	53.4	5.3	4.7	0.40	0.556	0.563
2003 216 – 220	51.0	0.6	52.9	3.6	3.8	0.32	0.557	0.566
2003 241 – 245	51.0	0.6	54.5	2.7	6.9	0.02	0.561	0.571
2003 275 – 279	51.0	0.6	51.3	5.4	0.6	0.90	0.558	0.557
2003 302 – 306	51.0	0.6	46.5	6.8	-8.8	0.15	0.558	0.546

Table 4: Probability of the retrieved space count value. Offset error and retrieved offset error are relative errors given in percent. Calibration coefficients are given in $\text{Wm}^{-2}\text{sr}^{-1}\mu\text{m}^{-1}/\text{DC}$.

5 VALIDATION

5.1 Radiance simulation accuracy estimation

BAND	MERIS	ATSR-2	SeaWiFS	VGT
BLUE	0.4	442	–	443
GREEN	0.5	560	550	555
RED	0.6	665	660	670
NIR	0.8	865	870	865
SWIR	1.6	–	–	MIR

Table 5: Selected spectral bands for each instrument.

The accuracy and precision of these simulations, *i.e.*, the reference against which SEVIRI is calibrated, have been evaluated comparing simulations with calibrated observations acquired by space-borne instruments (Govaerts and Clerici 2003). To this end, ERS2/ATSR-2, SeaStar/SeaWiFS, VEG-ETATION and Envisat/MERIS data have been collected over the desert targets simulated accounting for the actual observation conditions and spectral response of each instrument (Table 5). This analysis shows that the monthly mean relative bias between simulation and observation averaged over all targets remains low, but exhibits a small seasonal trend (Fig. 4). These results indicates that the reference can be used for the calibration of the SEVIRI solar channels with an expected accuracy of $\pm 5\%$ (Table 6) provided the calibration relies on the processing of a large number of observations. This error is lower than 3% in the SEVIRI VIS0.6 and VIS0.8 bands.

BAND	BLUE (0.4)			GREEN (0.5)			RED (0.6)			NIR (0.8)			SWIR (1.6)			
	SENSOR	r	$\bar{\beta}_m$	$\sigma_{\bar{\beta}_m}$	SENSOR	r	$\bar{\beta}_m$	$\sigma_{\bar{\beta}_m}$	SENSOR	r	$\bar{\beta}_m$	$\sigma_{\bar{\beta}_m}$	SENSOR	r	$\bar{\beta}_m$	$\sigma_{\bar{\beta}_m}$
ATSR2	–	–	–	0.94	-2.0	5.10	0.97	1.4	3.57	0.98	2.2	3.17	–	–	–	–
SeaWiFS	0.95	1.4	4.57	0.91	-2.0	4.78	0.96	-1.1	2.97	0.96	2.7	2.97	–	–	–	–
VGT	0.96	0.5	4.81	–	–	–	0.98	4.9	2.66	0.98	5.2	2.89	0.92	-4.1	4.95	–
MERIS	0.96	8.3	5.00	0.93	0.9	4.55	0.98	2.8	1.85	0.98	6.1	1.75	–	–	–	–

Table 6: Comparison between observations and simulations. r is the correlation coefficient. $\bar{\beta}_m$ is the mean relative bias in percent. $\sigma_{\bar{\beta}_m}$ is the standard error of $\bar{\beta}_m$.

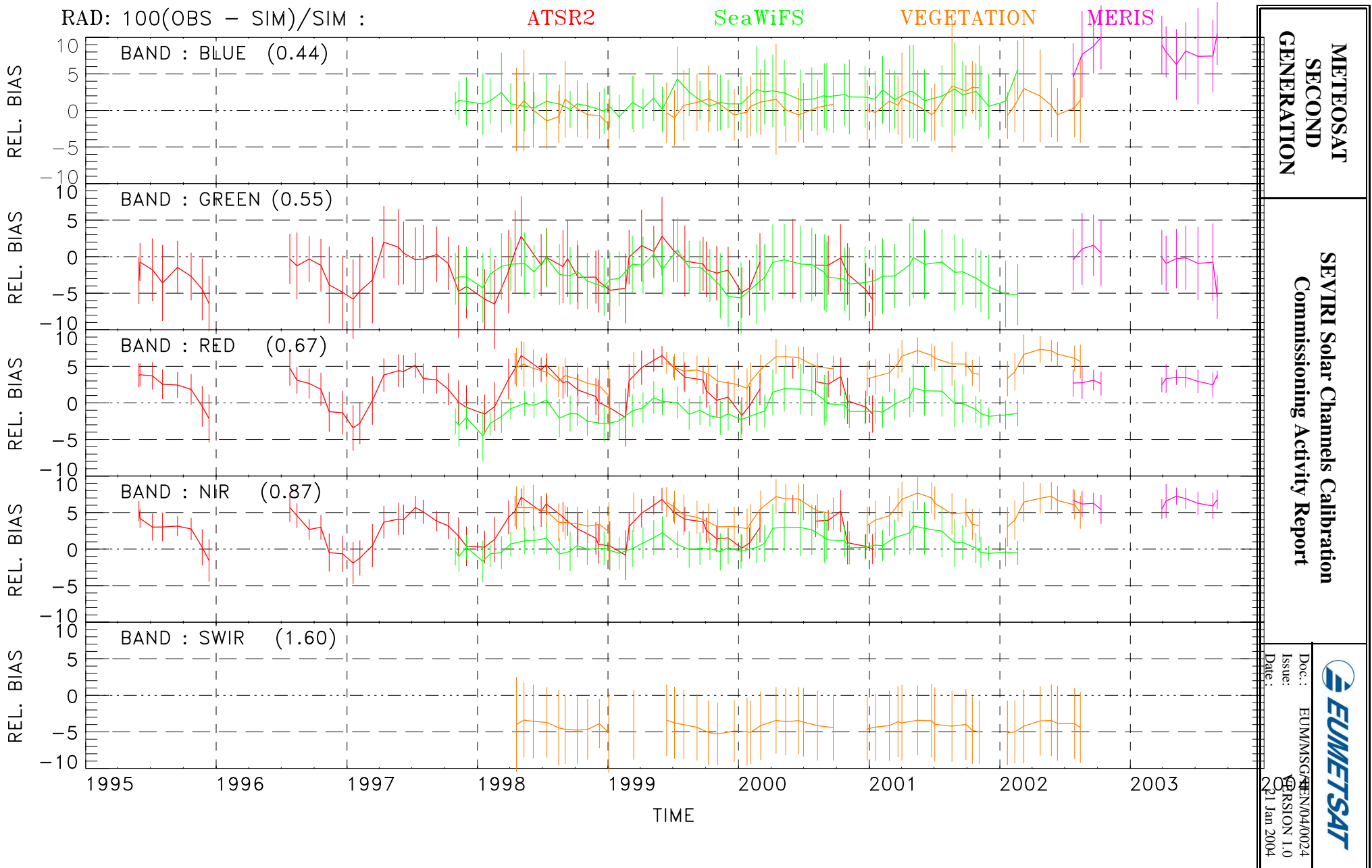


Figure 4: Monthly mean relative bias between observations and simulated radiances averaged over all desert targets in the blue, green, red, NIR and SWIR spectral regions. The standard error is shown with the vertical bars. The sensors are given the following color codes: ATSR-2 is in red, SeaWiFS in green, SPOT-4/VEGETATION in orange and MERIS in purple.

5.2 Comparison with CERES

The HRVIS band has been calibrated at RMIB using CERES radiance (August 2003) as calibration reference. The calibration coefficients have been derived over different two target types listed in Table (7).

Period	SCENE	NBR OBS	COEFF.	SSCC	REL. DIFF.
Aug. 2003	SEA	11496	0.563	0.530	-5.9%
Aug. 2003	BRIGHT DESERT	6931	0.539	0.557	+3.3%
Nov. 2003	SEA	1672	0.544	0.586	+7.7%
Nov. 2003	BRIGHT DESERT	4040	0.550	0.558	+1.5%

Table 7: Calibration coefficients derived with CERES over sea and bright desert targets in comparison with the SSCC values. Coefficients are given in $\text{Wm}^{-2}\text{sr}^{-1}\mu\text{m}^{-1}/\text{DC}$.

Results over bright desert targets show that the average estimated calibration error for the HRVIS band (4.5%, Table 3) is fairly realistic.

6 APPLYING THE CALIBRATION COEFFICIENTS

This section describes the various processing steps to apply the calibration coefficients stored in the Level 1.5 images to transform the digital count in radiance and reflectance factor. The calibration coefficients c_f and offset values R_0 are stored in the fields `cal_slope` [$\text{mWm}^{-2}\text{sr}^{-1}(\text{cm}^{-1})^{-1}/\text{DC}$] and `cal_offset` [$\text{mWm}^{-2}\text{sr}^{-1}(\text{cm}^{-1})^{-1}$] of the SEVIRI level 1.5 native format in the file header: `RADIOMETERPROCESSING.Level1_5ImageCalibration` (refer to document EUM/MSG/ICD/105).

BAND	$\tilde{\xi}$ μm	λ_0 μm	I_μ $\text{Wm}^{-2}\mu\text{m}^{-1}$	I_m $\text{mWm}^{-2}(\text{cm}^{-1})^{-1}$
VIS06	0.0744803	0.635	1618.0	65.2296
VIS08	0.0572863	0.810	1113.0	73.0127
NIR	0.1256780	1.640	231.9	62.3715
HRVIS	0.4220080	0.750	1403.0	78.8952

Table 8: Relevant ancillary information for the level 1.5 MSG-1/SEVIRI data. $\tilde{\xi}$ is the integral value of the NSR. λ_0 is the central wavelength of the band. I_μ and I_m are the band solar irradiance at 1 AU expressed in two different units.

The transformation of the level 1.5 count value K [DC] in radiance R_m [$\text{mWm}^{-2}\text{sr}^{-1}(\text{cm}^{-1})^{-1}$] is given by

$$R_m = c_f K + R_0 \quad (1)$$

where R_0 has a negative value in the file header. If needed, this radiance can be converted in [$\text{Wm}^{-2}\text{sr}^{-1}\mu\text{m}^{-1}$] with

$$R_\mu = \frac{10 R_m}{\lambda_0^2} \quad (2)$$

The transformation of radiances R_m or R_μ acquired at time t in a given location \vec{x} into Bidirectional Reflectance Factor (BRF) r [unitless] is given by

$$r = \frac{\pi R_m d^2(t)}{I_m \cos(\theta_s(t, \vec{x}))} = \frac{\pi R_\mu d^2(t)}{I_\mu \cos(\theta_s(t, \vec{x}))} \quad (3)$$

where $d^2(t)$ is the actual Sun-Earth distance [AU] at time t and $\theta_s(t, \vec{x})$ is the Sun Zenith Angle [rad] at time t and location \vec{x} .

7 CONCLUSION

The calibration reference used for the operational vicarious calibration of the SEVIRI solar channels consists of simulated TOA radiances over bright desert targets, using a data set of surface and atmospheric properties. The accuracy and precision evaluation of this reference relies on a comparison between calibrated spaceborne data and their simulation. These comparisons reveal that the relative bias between simulations and calibrated observations does not exceed 3% in the VIS0.6 and VIS0.8 bands with respect to ATSR-2 and SeaWiFS, when a large number of observation are averaged over all targets.

The SSCC algorithm has already been successfully applied for the calibration of the SEVIRI solar channels during commissioning. The estimated calibration error is lower to 5% for each band and is consistent with the accuracy estimation of the radiative transfer modelling and the comparison with CERES cross-calibration.

Within the SSCC accuracy limit, it has not been possible to detect any anomaly in the NSR characterization, the linearity of the response or the characterization of the offset value.

The duration of the commissioning period was not long enough to estimate the drift of the instrument. The solar channels appear however radiometrically very stable.

References

- Govaerts, Y. M. and M. Clerici (2003). Evaluation of radiative transfer simulations over bright desert calibration sites. *IEEE Transactions on Geoscience and remote sensing in print*.
- Govaerts, Y. M., B. Pinty, M. M. Verstraete, and J. Schmetz (1998). Exploitation of angular signatures to calibrate geostationary satellite solar channels. In IEEE (Ed.), *IGARSS'98*, Seattle, USA, pp. 327–329.
- Koepke, P. (1982). Vicarious satellite calibration in the solar spectral range by means of calculated radiances and its application to Meteosat. *Applied Optics* 21, 2845–2854.
- Müller, J. (2003). Msg system commissioning: Calibration validation plan. Technical Report EUMMSGPLN169, EUMETSAT.
- Schmetz, J., P. Pili, S. Tjemkes, D. Just, J. Kerkmann, S. Rota, and A. Ratier (2002). An introduction to Meteosat Second Generation. *Bulletin of the American Meteorological Society* 83, 977–992.
- Vermote, E. F., D. Tanré, J. L. Deuzé, M. Herman, and J. J. Morcrette (1997). Second simulation of the satellite signal in the solar spectrum, 6S: An overview. *IEEE Transactions on Geoscience and Remote Sensing* 35, 675–686.

**METEOSAT
SECOND
GENERATION**

**SEVIRI Solar Channels Calibration
Commissioning Activity Report**



Doc. : EUM/MSG/TEN/04/0024
Issue: VERSION 1.0
Date : 21 Jan 2004

Annex

A HRVIS SPECTRAL RESPONSE USED IN SSCC

LAMBDA	TRANSMIT	ERROR	LAMBDA	TRANSMIT	ERROR
0.3	0.0	0.0000	0.805	0.937729	0.0236
0.305	0.0	0.0000	0.81	0.928404	0.0232
0.31	0.0	0.0000	0.815	0.917732	0.0227
0.315	0.0	0.0000	0.82	0.905102	0.0222
0.32	0.0	0.0000	0.825	0.889974	0.0217
0.325	0.0	0.0000	0.83	0.874472	0.0214
0.33	0.0	0.0000	0.835	0.859877	0.0208
0.335	0.0	0.0000	0.84	0.843129	0.0201
0.34	0.0	0.0000	0.845	0.823579	0.0194
0.345	0.0	0.0000	0.85	0.801977	0.0187
0.35	0.0	0.0000	0.855	0.779172	0.0182
0.355	0.0	0.0000	0.86	0.757268	0.0178
0.36	0.0	0.0000	0.865	0.737092	0.0171
0.365	0.0	0.0000	0.87	0.715657	0.0165
0.37	0.0	0.0000	0.875	0.693762	0.0158
0.375	0.0	0.0006	0.88	0.670357	0.0151
0.38	0.00648999	0.0036	0.885	0.645769	0.0145
0.385	0.0358778	0.0067	0.89	0.621828	0.0137
0.39	0.0648286	0.0097	0.895	0.596449	0.0118
0.395	0.0933429	0.0127	0.9	0.558215	0.0114
0.4	0.12142	0.0156	0.905	0.52593	0.0127
0.405	0.14906	0.0182	0.91	0.501767	0.0135
0.41	0.176264	0.0206	0.915	0.47961	0.0141
0.415	0.20303	0.0224	0.92	0.457653	0.0146
0.420	0.224800	0.0245	0.925	0.435748	0.0148
0.425	0.250448	0.0263	0.93	0.412754	0.0151
0.430	0.273588	0.0284	0.935	0.39051	0.0152
0.435	0.301199	0.0302	0.94	0.368914	0.0153
0.440	0.327159	0.0314	0.945	0.347842	0.0153
0.445	0.348259	0.0335	0.95	0.327196	0.0151
0.45	0.377908	0.0350	0.955	0.306704	0.0148
0.455	0.404348	0.0364	0.96	0.285726	0.0144
0.46	0.429666	0.0374	0.965	0.264278	0.0139
0.465	0.452927	0.0382	0.97	0.243716	0.0134
0.47	0.474291	0.0389	0.975	0.223566	0.0128
0.475	0.494633	0.0395	0.98	0.204392	0.0122
0.48	0.515154	0.0400	0.985	0.186587	0.0115
0.485	0.535834	0.0404	0.99	0.169176	0.0110
0.49	0.555156	0.0402	0.995	0.154513	0.0107
0.495	0.570411	0.0393	1	0.143659	0.0104
0.5	0.577475	0.0381	1.005	0.134201	0.0101
0.505	0.579319	0.0384	1.01	0.125228	0.0097
0.51	0.594507	0.0383	1.015	0.116691	0.0094
0.515	0.610841	0.0381	1.02	0.108776	0.0090
0.52	0.626467	0.0377	1.025	0.101707	0.0087
0.525	0.64123	0.0372	1.03	0.0952497	0.0084
0.53	0.655506	0.0367	1.035	0.0889682	0.0081
0.535	0.669956	0.0362	1.04	0.083024	0.0078
0.54	0.685283	0.0359	1.045	0.0776488	0.0075
0.545	0.702662	0.0353	1.05	0.0726208	0.0070
0.55	0.719514	0.0347	1.055	0.0655695	0.0064
0.555	0.73694	0.0340	1.06	0.0605224	0.0059
0.56	0.754121	0.0332	1.065	0.0557832	0.0054
0.565	0.769855	0.0321	1.07	0.0513402	0.0050
0.57	0.784086	0.0309	1.075	0.047181	0.0046
0.575	0.796048	0.0298	1.08	0.0432938	0.0042
0.58	0.808254	0.0286	1.085	0.0396663	0.0039
0.585	0.820008	0.0273	1.09	0.0362867	0.0035
0.59	0.830925	0.0260	1.095	0.0331432	0.0032
0.595	0.840909	0.0246	1.1	0.0302239	0.0029
0.6	0.850145	0.0234	1.105	0.0275176	0.0027
0.605	0.861487	0.0236	1.11	0.0250127	0.0024
0.61	0.87237	0.0237	1.115	0.0226984	0.0022
0.615	0.881282	0.0238	1.12	0.0205637	0.0020
0.62	0.88876	0.0240	1.125	0.0185983	0.0018
0.625	0.896124	0.0242	1.13	0.0167918	0.0016
0.63	0.904216	0.0246	1.135	0.0151344	0.0014
0.635	0.913579	0.0247	1.14	0.0136165	0.0013
0.64	0.921252	0.0247	1.145	0.012229	0.0012
0.645	0.927665	0.0249	1.15	0.010963	0.0010
0.65	0.933962	0.0251	1.155	0.00981	0.0009
0.655	0.940742	0.0252	1.16	0.00876199	0.0008
0.66	0.946811	0.0253	1.165	0.00781122	0.0007
0.665	0.952234	0.0256	1.17	0.00695034	0.0007
0.67	0.959581	0.0260	1.175	0.00617241	0.0006
0.675	0.9688	0.0259	1.18	0.00547083	0.0005
0.68	0.974913	0.0255	1.185	0.00483939	0.0005
0.685	0.974768	0.0254	1.19	0.00427224	0.0004
0.69	0.97378	0.0257	1.195	0.00376391	0.0004
0.695	0.975839	0.0258	1.2	0.00330924	0.0003
0.7	0.978607	0.0261	1.205	0.00290344	0.0003
0.705	0.983441	0.0261	1.21	0.00254203	0.0002
0.71	0.987417	0.0259	1.215	0.00222085	0.0002
0.715	0.988267	0.0260	1.22	0.00193607	0.0002
0.72	0.989315	0.0261	1.225	0.0016841	0.0002
0.725	0.991133	0.0261	1.23	0.00146169	0.0001
0.73	0.993019	0.0262	1.235	0.0012658	0.0001
0.735	0.995486	0.0263	1.24	0.00109368	0.0001

0.74	0.998207	0.0262	1.245	0.000942785	0.0001
0.745	0.999549	0.0259	1.25	0.000810823	0.0001
0.75	0.997296	0.0259	1.255	0.000695689	0.0001
0.755	0.99563	0.0256	1.26	0.000595483	0.0001
0.76	0.99163	0.0255	1.265	0.00050848	0.0000
0.765	0.987021	0.0251	1.27	0.000433129	0.0000
0.77	0.979765	0.0245	1.275	0.000368033	0.0000
0.775	0.968345	0.0241	1.28	0.00031194	0.0000
0.78	0.956045	0.0246	1.285	0.000263726	0.0000
0.785	0.952065	0.0249	1.29	0.000222394	0.0000
0.79	0.951805	0.0246	1.295	0.000187055	0.0000
0.795	0.948947	0.0243	1.3	0.000156918	0.0000
0.8	0.943745	0.0241			

B ERROR BUDGET OVER SEA TARGETS

	ATM	SRF	RTM	NSR	NOISE	RAND.	TOT.
SEA VIS06							
OBSERV. $\delta_r c_f$	16.1		2.4	1.0	0.4		16.4
TIME AVG. $\delta_r \bar{c}_f$	19.2		3.1	1.2		6.4	21.2
SPACE AVG. $\delta_r \hat{\bar{c}}_f$			3.2	1.3		17.7	18.1
SEA HRV							
OBSERV. $\delta_r c_f$	15.1		2.6	1.7	0.4		15.4
TIME AVG. $\delta_r \bar{c}_f$	18.4		3.2	2.2		2.3	19.1
SPACE AVG. $\delta_r \hat{\bar{c}}_f$			3.4	2.3		27.1	27.4

Table 9: Relative error (%) contribution on the estimation of the calibration coefficient over sea targets.

C METEOSAT-7 ERROR BUDGET

	ATM	SRF	RTM	NSR	NOISE	RAND.	TOT.
DESERT							
OBSERV. $\delta_r c_f$	1.8	12.4	4.1	3.8	0.9		13.9
TIME AVG. $\delta_r \bar{c}_f$	1.9	12.5	4.2	3.8		0.4	13.9
SPACE AVG. $\delta_r \hat{\bar{c}}_f$			4.1	3.8		1.6	5.9
SEA							
OBSERV. $\delta_r c_f$	8.6		3.1	7.7	2.8		12.0
TIME AVG. $\delta_r \bar{c}_f$	8.7		3.2	7.7		2.3	12.4
SPACE AVG. $\delta_r \hat{\bar{c}}_f$			3.2	7.7		3.0	8.9

Table 10: Relative error (%) contribution on the estimation of the calibration coefficient over desert and sea targets for Meteosat-7.

**METEOSAT
SECOND
GENERATION**

**SEVIRI Solar Channels Calibration
Commissioning Activity Report**



Doc. : EUM/MSG/TEN/04/0024
Issue: VERSION 1.0
Date : 21 Jan 2004

D CALIBRATION RESULTS OVER EACH TARGET

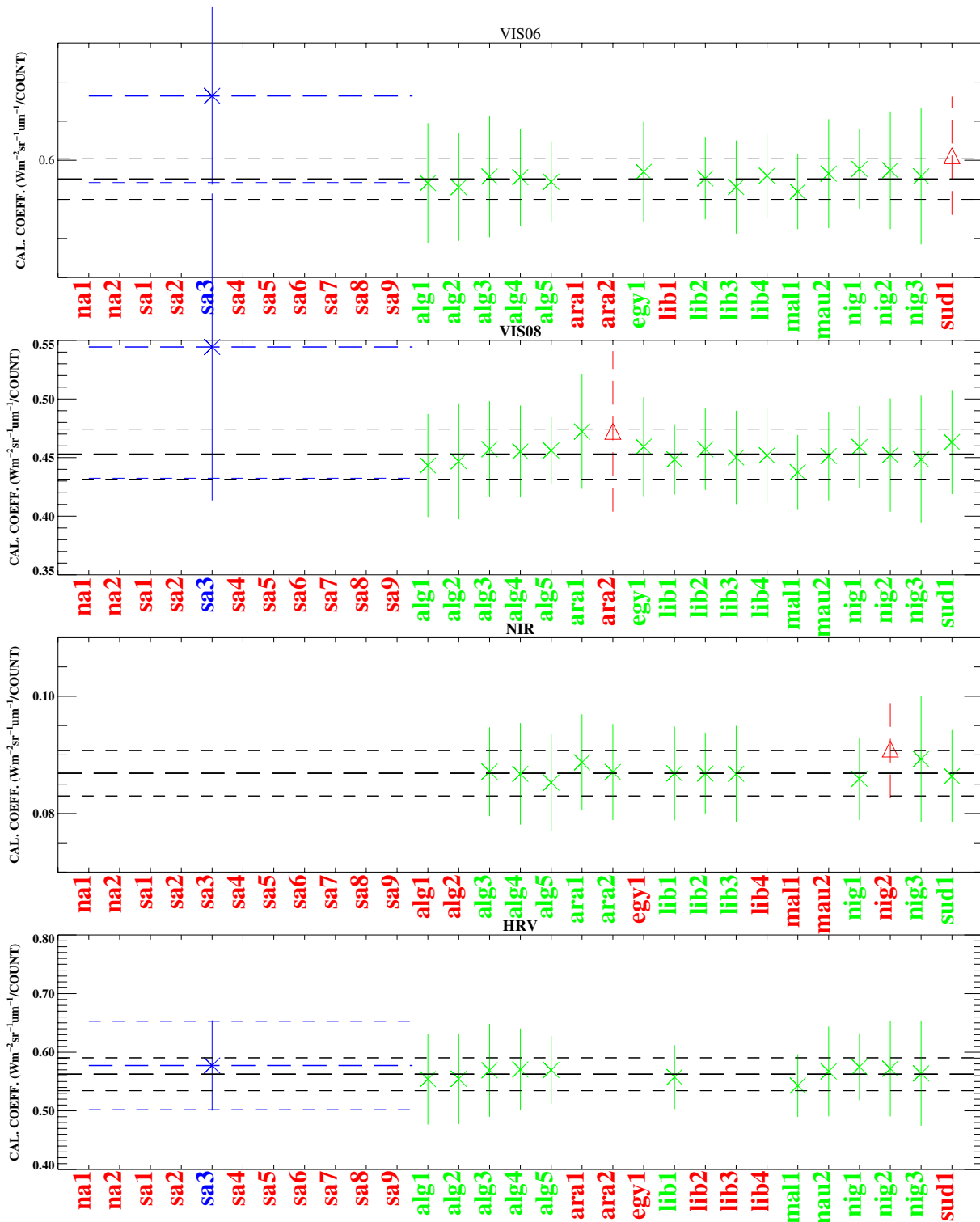


Figure 5: Calibration results over each target for RUNID: MSG1_2003_054_3.06.

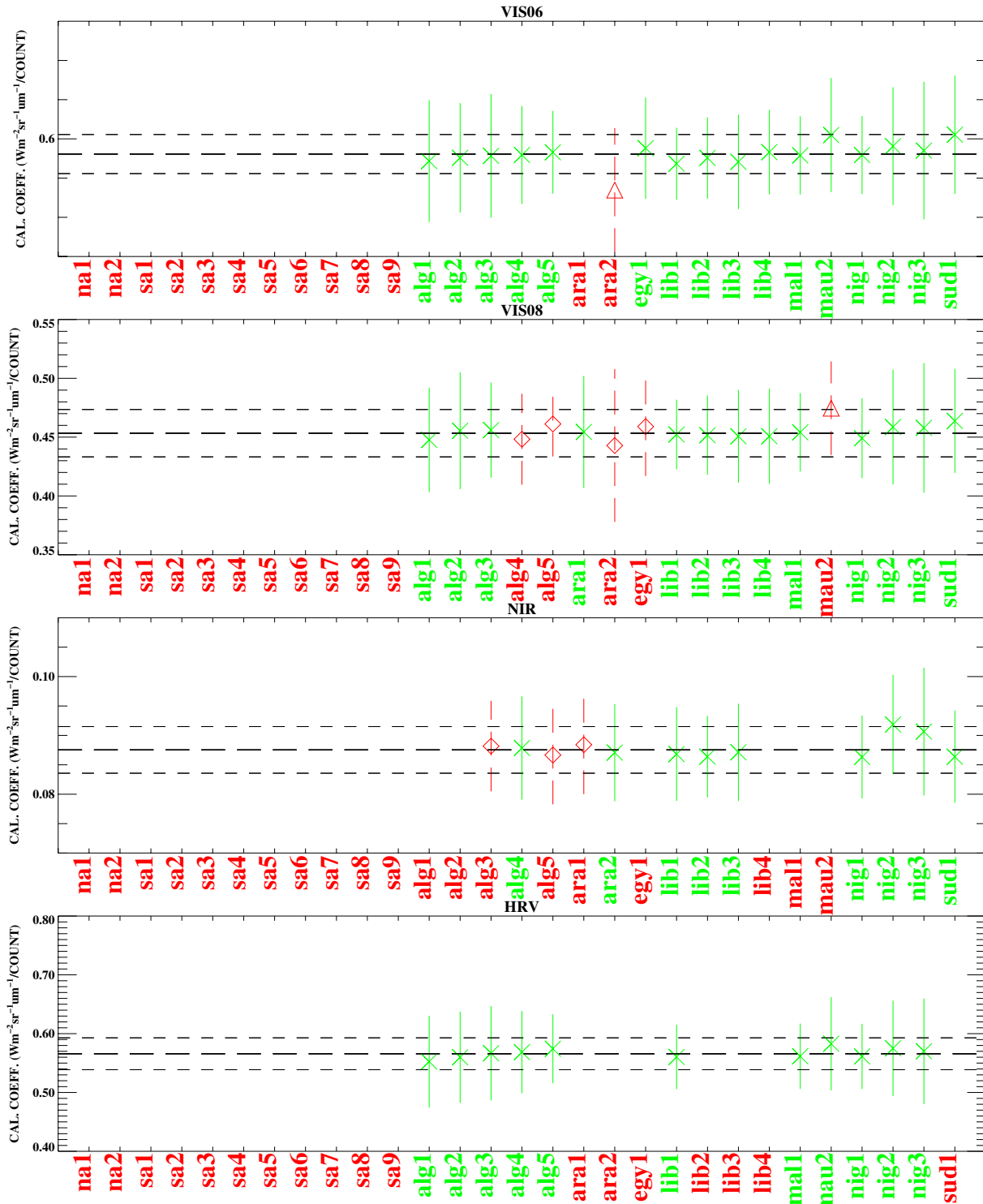


Figure 6: Calibration results over each target for RUNID: MSG1_2003_073_3.06.

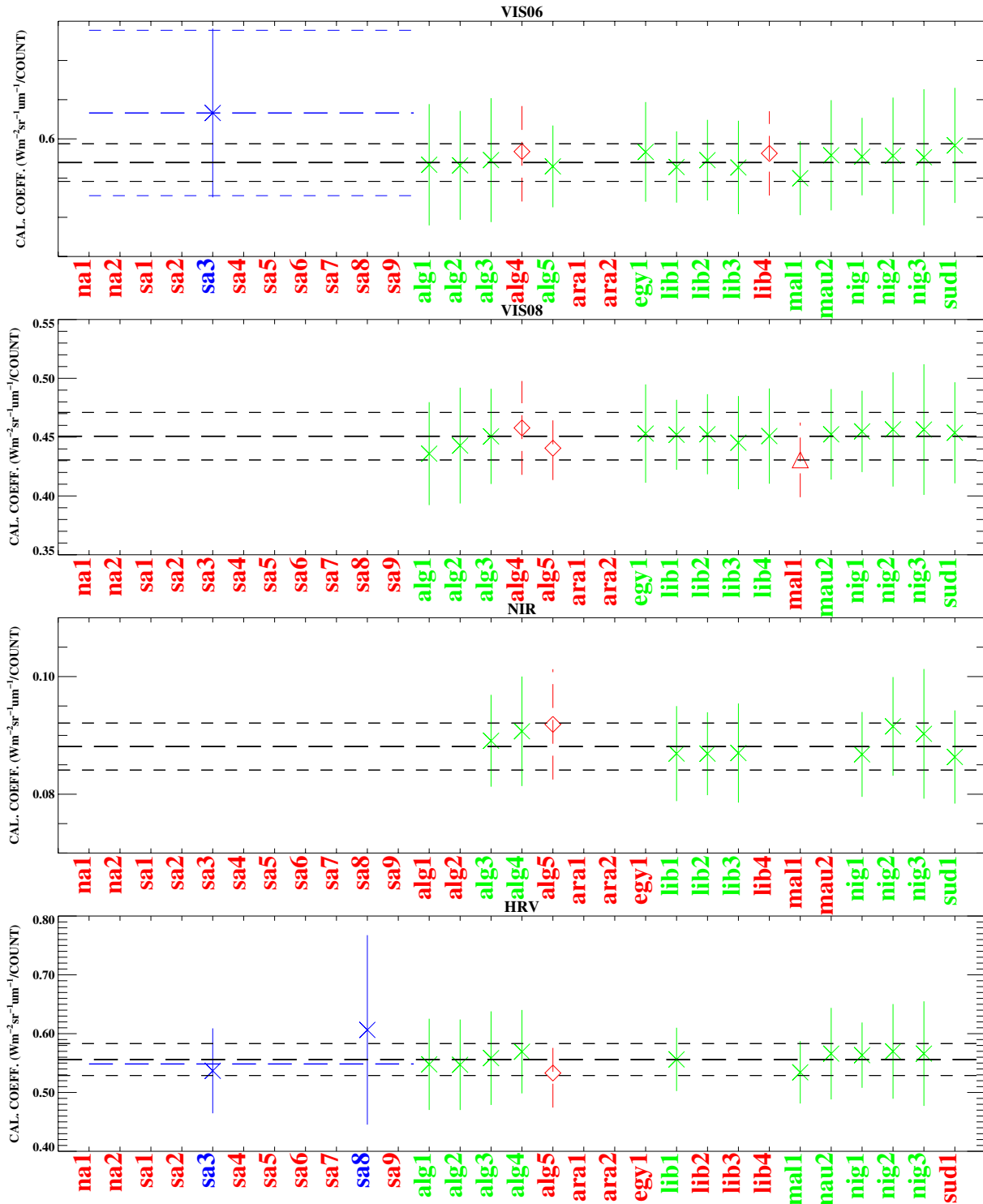


Figure 7: Calibration results over each target for RUNID: MSG1_2003_086_3.06.

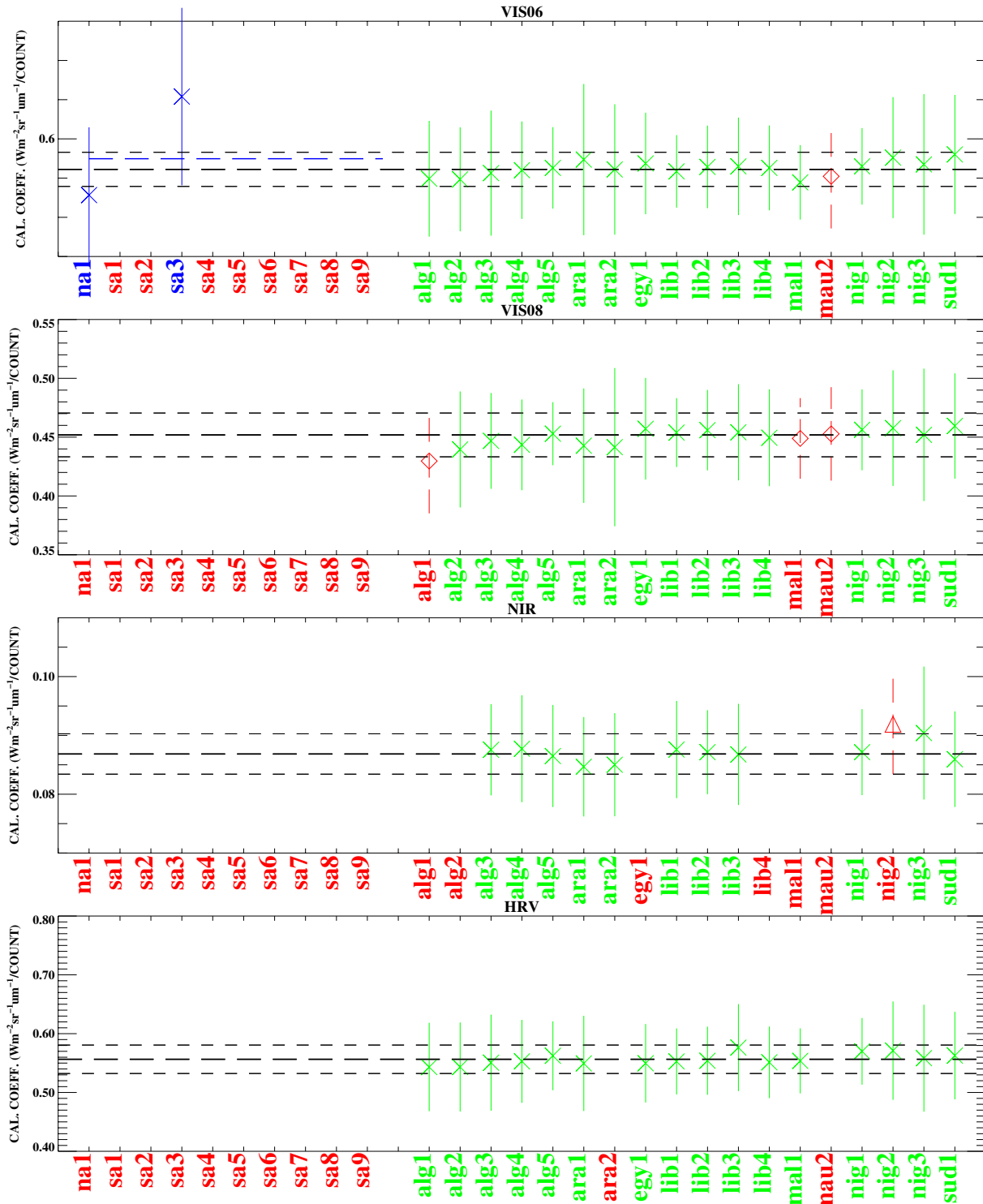


Figure 8: Calibration results over each target for RUNID: MSG1_2003_199_3.06.

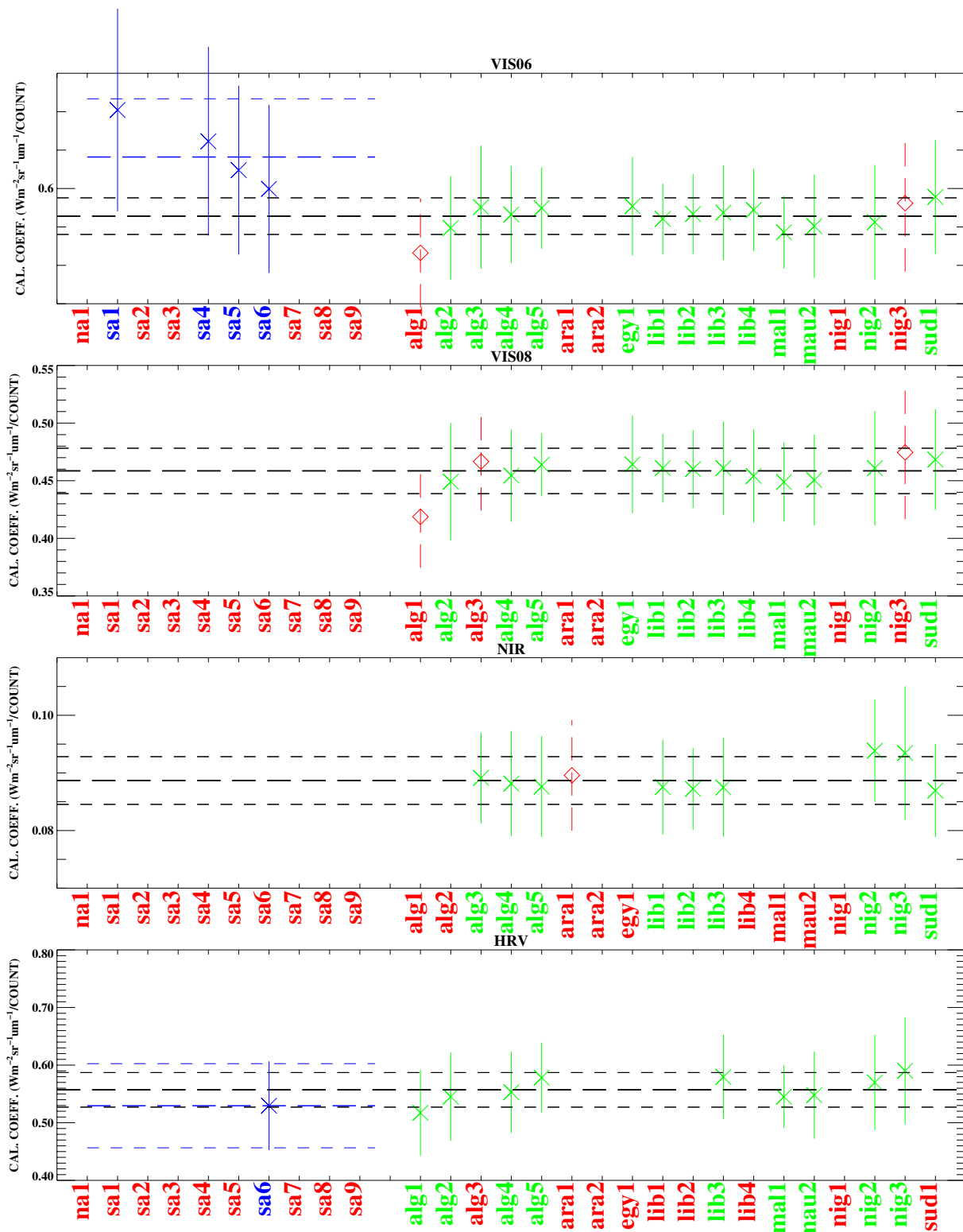


Figure 9: Calibration results over each target for RUNID: MSG1_2003_216_3.06.

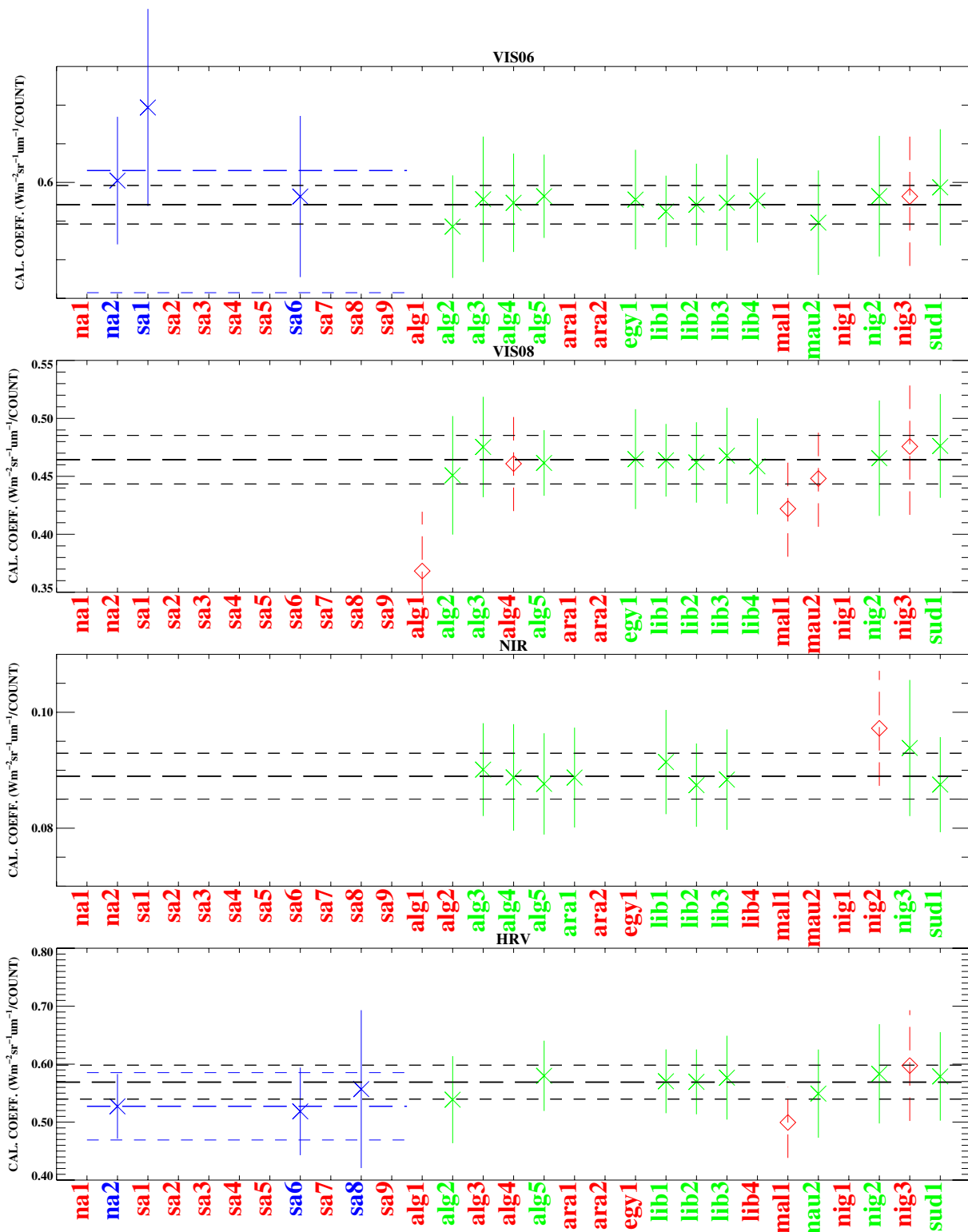


Figure 10: Calibration results over each target for RUNID: MSG1_2003_216_220_IQGSE.

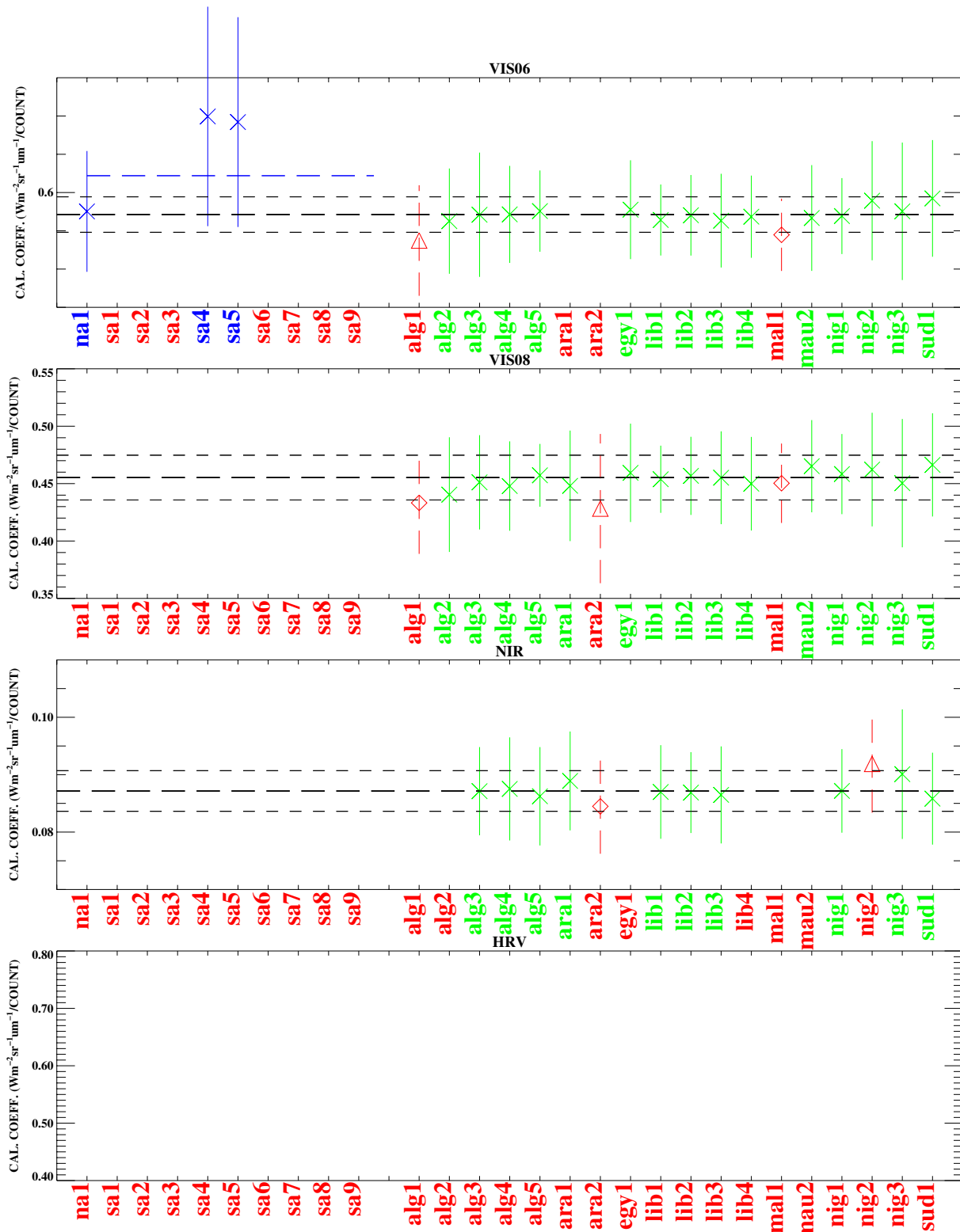


Figure 11: Calibration results over each target for RUNID: MSG1_2003_234_3.06.

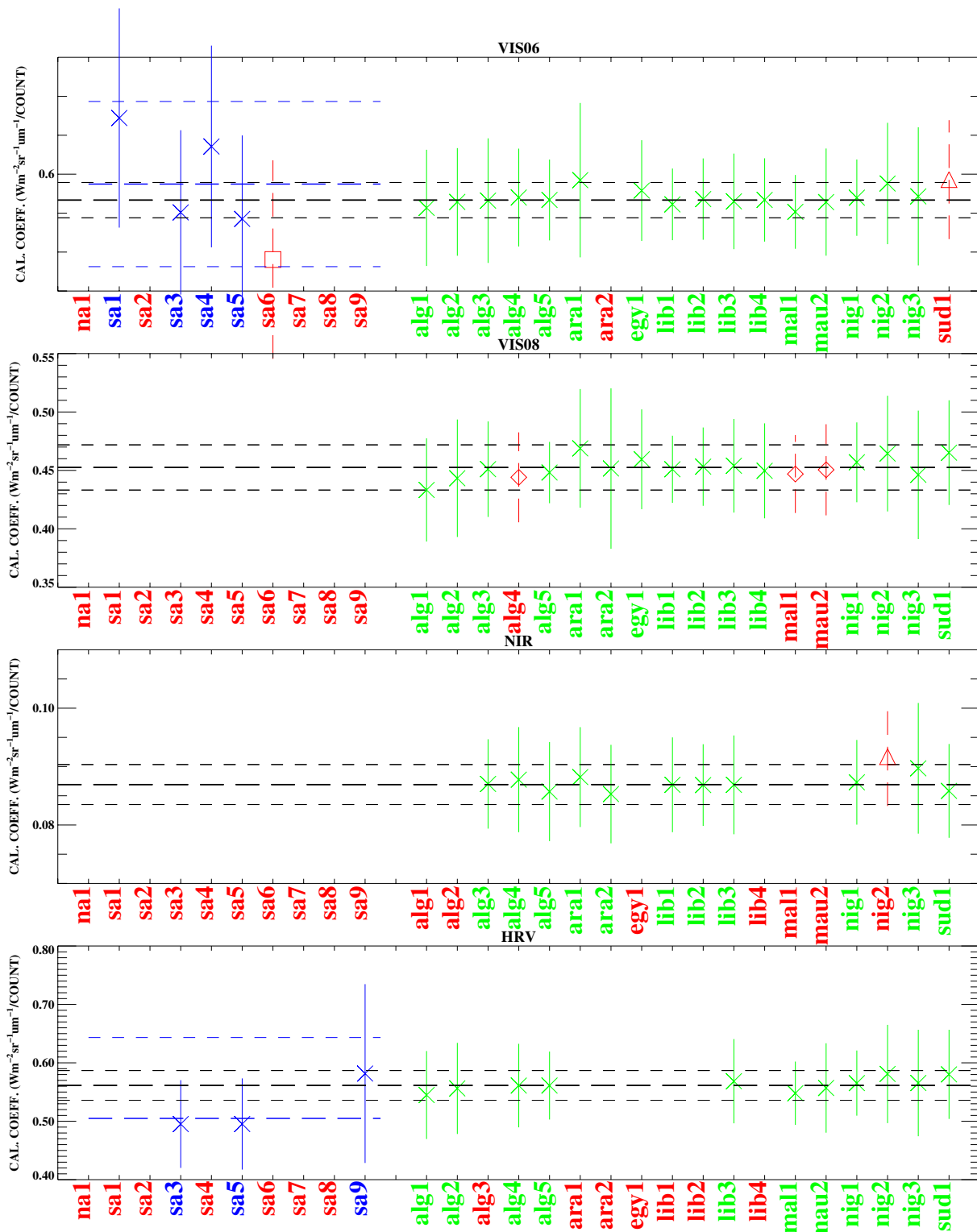


Figure 12: Calibration results over each target for RUNID: MSG1_2003_241_3.06.

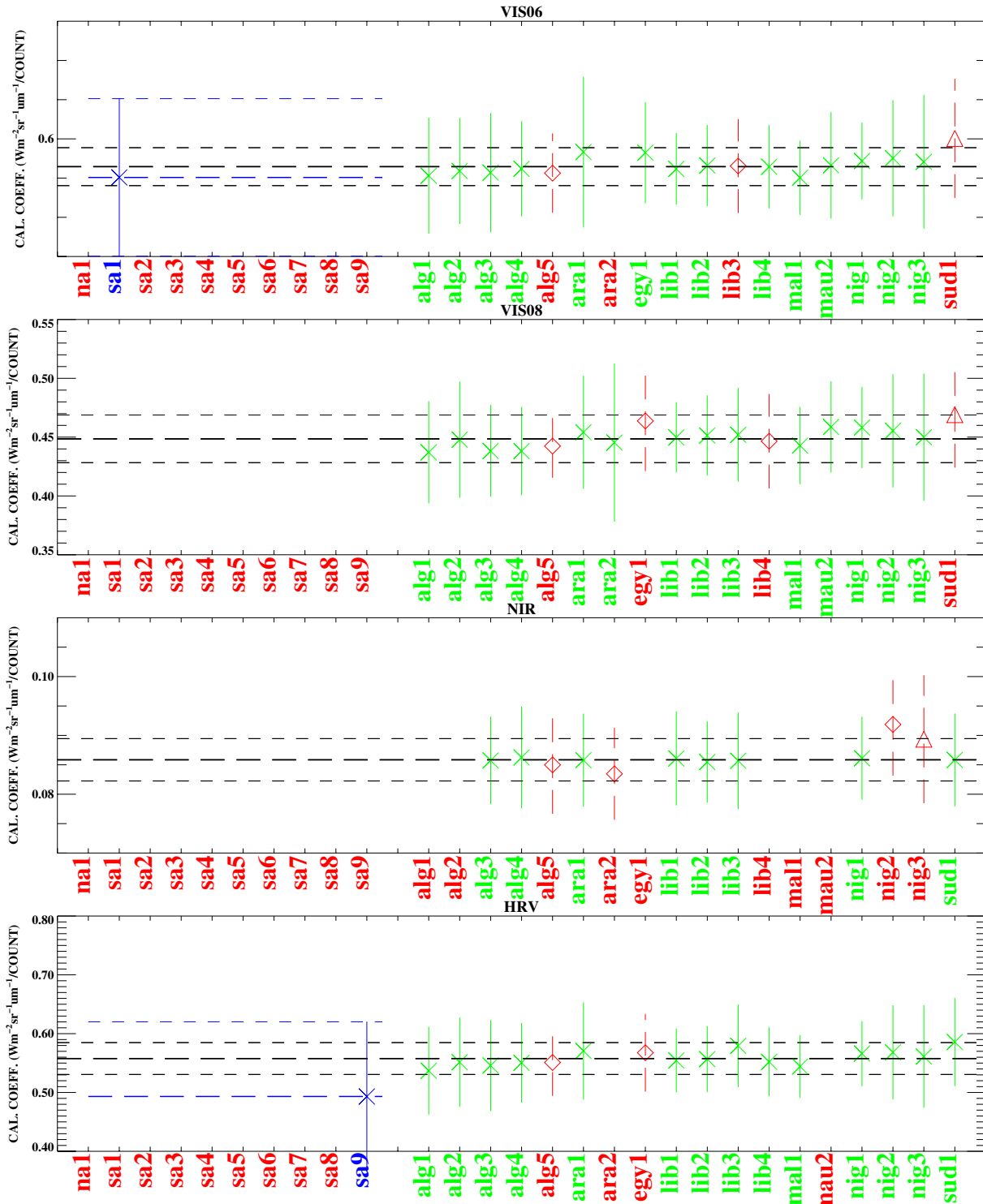


Figure 13: Calibration results over each target for RUNID: MSG1_2003_275_3.06.

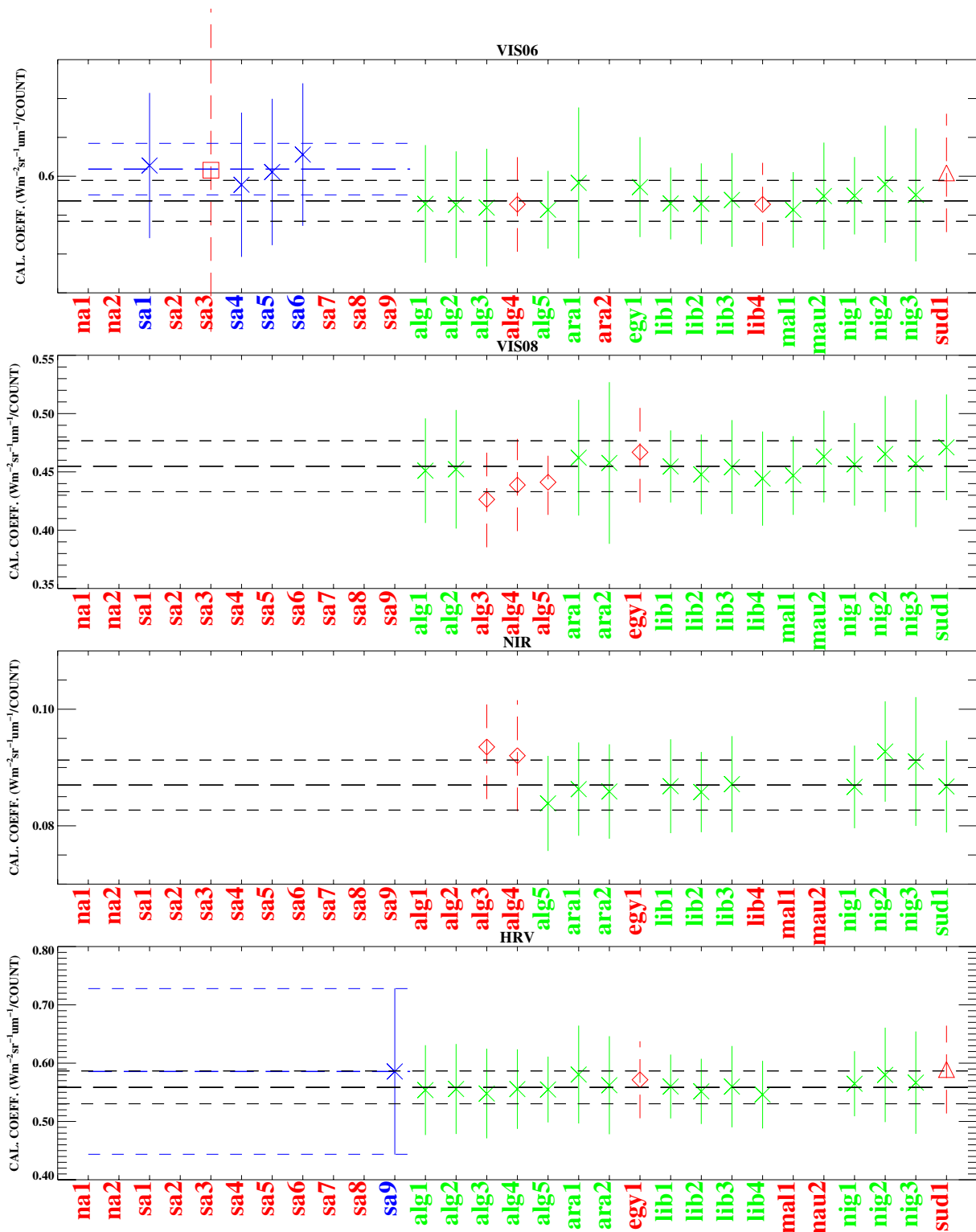


Figure 14: Calibration results over each target for RUNID: MSG1_2003_302_3.06.